Quantum Electronics **51** (9) 759–767 (2021)

https://doi.org/10.1070/QEL17620

Design of the front-end system for a subexawatt laser of the XCELS facility

I.B. Mukhin, A.A. Soloviev, E.A. Perevezentsev, A.A. Shaykin, V.N. Ginzburg, I.V. Kuzmin, M.A. Mart'yanov, I.A. Shaikin, A.A. Kuzmin, S.Yu. Mironov, I.V. Yakovlev, E.A. Khazanov

Abstract. **A concept of the front-end system of the XCELS (eXawatt Center for Extreme Light Studies) facility is presented. Its design is aimed at achieving high stability of laser radiation parameters and possibility of their control in a wide range. Optically synchronised chirped signal (wavelength 910 nm, bandwidth more than 100 nm, and duration ~3 ns) and pump (wavelength 1054 nm, bandwidth ~1 nm, and duration ~4 ns) pulses for XCELS parametric amplifiers will be implemented at the output of the front-end system. Chirped femtosecond pulses with energies above 100 mJ [no more than 15 fs long after compression, with carrier-envelope phase (CEP) stabilisation] will have a repetition rate up to 100 Hz, which will allow one to implement active energy stabilisation and to minimise the angular jitter of the emitted beam at the XCELS output. The application of picosecond pumping in the parametric amplifier of the front-end system should provide a high contrast of femtosecond pulses. The pump pulse will be linearly frequency-modulated; this approach will not affect the parametric amplification efficiency but make it possible to use spectral methods to control the pump pulse shape in order to form a pulse of specified shape at the output of power amplifiers, even under conditions of their strong saturation.**

Keywords: *femtosecond lasers, ultra-high-power lasers, XCELS, parametric amplification, optical synchronisation, pulse shape control.*

1. Introduction

The achievement of peak laser intensities above 10^{24} W cm^{-2} opens a unique possibility of studying such new fundamental processes as vacuum polarisation, generation of elementary particles, etc. Specifically for this reason the scientific community is actively involved in the development of increasingly higher power lasers, thus blazing a path to a new direction in experimental physics. To date, using different approaches, a peak power level of several PW has been achieved: 4.8-PW power was obtained based on optical parametric chirped pulse amplification (OPCPA) [1]. Chirped pulse amplification (CPA) was used to obtain a peak power of 10 PW in Ti:sapphire crystals [2]. The use of CPA also provided a petawatt power level in neodymium- or ytterbium-activated laser media [3, 4]. Some other ways to increase the peak power of petawatt lasers based on nonlinear interaction of radiation with a medium were considered [5, 6].

To date, all projects aimed at scaling peak power to a level of 100 PW imply specifically OPCPA in wide-aperture DKDP crystals, because they possess a large aperture and unique ultrabroadband phase matching at a wavelength of 910 nm [7]. For example, the researchers from the Rochester Laboratory for Laser Energetics (LLE) proposed to use channels of the OMEGA system to pump the ultraintense parametric system EP-OPAL [8]. It is planned to achieve a power of 30 PW in two channels, which would provide (after double focusing) intensities higher than 10^{23} W cm^{-2}. A GEKKO-EXA project was proposed at the Institute of Laser Engineering (ILE), Osaka University [9], whose goal is to attain a power of 50 PW using the radiation from one of the LFEX channels for pumping. A SEL laser with a peak power up to 100 PW, based on coherent addition of four channels with a power of 30 PW per each, is being developed at the Shanghai Institute of Optics and Fine Mechanics (SIOM) [10]. Another project carried out at this institute, SG-II [11], implies addition of six parametric channels with a total peak power of 250 PW, which should provide (after focusing) an intensity of 10^{25} W cm^{-2}.

One of such projects is XCELS [12], which also involves ultrabroadband parametric amplification of 910-nm radiation in a DKDP crystal and a multichannel architecture based on the technology of coherent pulse addition. An important feature of the XCELS facility is the application of dipole geometry for focusing [13], which yields a maximum electric field amplitude in the focus. The system suggests coherent addition of 12 femtosecond power channels with a power of ~15 PW per each, which should provide a radiation intensity of 10^{25} W cm^{-2} in the interaction region. The concept of coherent addition imposes exceptionally stringent requirements on the stability of all parameters of the facility, which must be ensured in all stages, from the generation and preliminary amplification of a seed pulse in the front-end system to the compression and focusing in the target chamber.

In this study we present a conceptual design of the front-end system of Mega Science XCELS facility. The main requirements to the output parameters of the front-end system are formulated, and ways to fulfil them (based on experimental experience) are proposed.

I.B. Mukhin, A.A. Soloviev, E.A. Perevezentsev, A.A. Shaykin, V.N. Ginzburg, I.V. Kuzmin, M.A. Martyanov, I.A. Shaikin, A.A. Kuzmin, S.Yu. Mironov, I.V. Yakovlev, E.A. Khazanov Institute of Applied Physics, Russian Academy of Sciences, ul. Ul'yanova 46, 603950 Nizhny Novgorod, Russia; e-mail: mib_1982@mail.ru

Received 17 April 2021; revision received 11 August 2021
Kvantovaya Elektronika **51** (9) 759–767 (2021)
Translated by Yu.P. Sin'kov

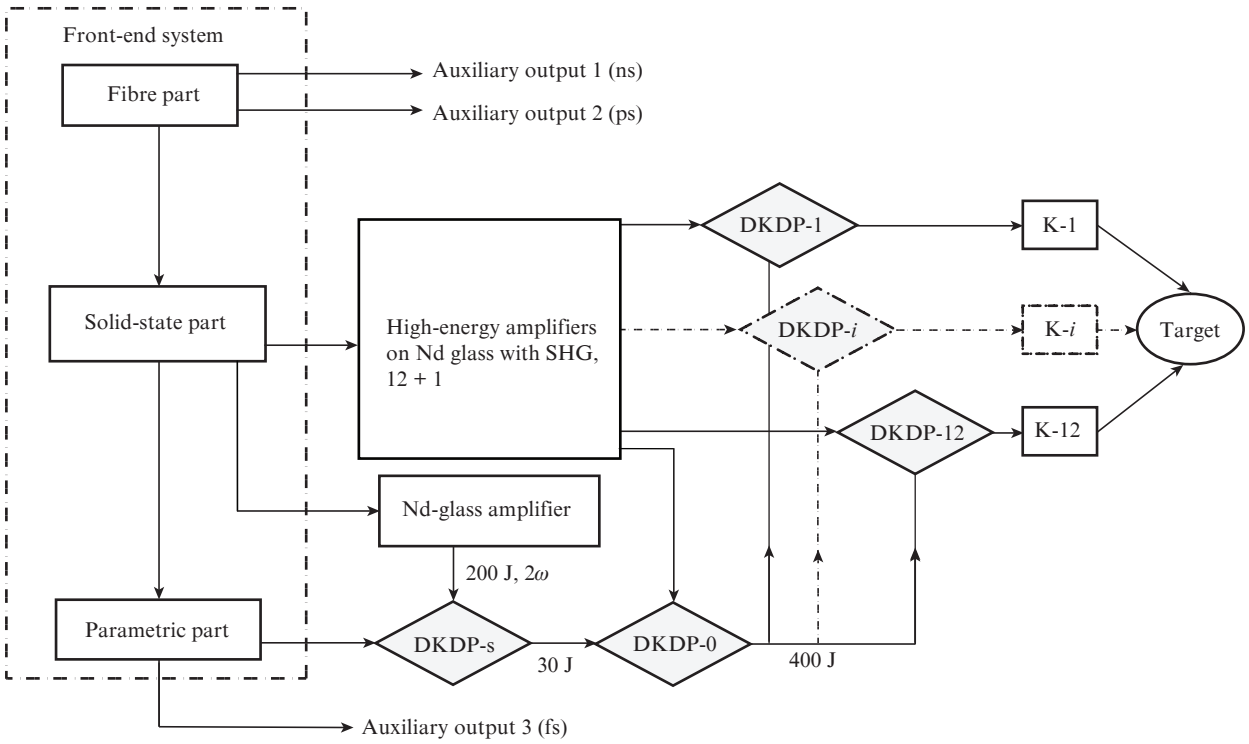

Figure 1. Functional scheme of XCELS.

2. Requirements to the XCELS front-end system

The functional scheme of the XCELS complex is shown in Fig. 1. Its front-end system (outlined by dashed lines) should provide synchronous generation of injection pulse to Nd:glass amplifiers (pump beam, $\lambda = 1054$ nm [14]) and a broadband signal injection pulse to the OPCPA amplifiers based on a DKDP crystal (signal beam, $\lambda = 910$ nm). After preliminary amplification (DKDP-s and DKDP-0 amplifiers), the signal beam is divided into 12 channels, each consisting of a final amplifier (DKDP-1-12) and a compressor (C-1-12). Either the amplifier developed at the Institute of Applied Physics RAS [15] or a commercial amplifier [16] can be used to pump DKDP-s. High-energy Nd:glass amplifiers for pumping DKDP-0-12 are similar to those used in the UFL-2M project [17]. The payment for the use of ultrabroadband parametric amplification (with further coherent addition of channels) is the exceptionally stringent requirements to the signal jitter relative to pumping, which can be satisfied only based on optical synchronisation. The requirement to the pump pulse duration is determined by the duration of the chirped signal pulse, which, in turn, is specified by the stretcher–compressor system. The durations of pump and signal pulses in XCELS are approximately 4 and 3 ns, respectively.

The femtosecond signal pulses at the output of the front-end system should have a fairly high energy and sufficiently high repetition rate to ensure both their further efficient parametric amplification and possibility of active energy and wavefront stabilisation in the next 12 amplification channels and in the target chamber. In addition, the optical contrast of femtosecond pulse should satisfy more than enough the requirements to the contrast of the output pulse of the entire laser facility ($\sim 10^{12}$). The parameters of the pulse injected into high-energy pump lasers should be variable in wide ranges to allow the amplification modes to be optimised and the temporal shape of laser pulse to be controlled. It is planned to maintain high stability of the main parameters of the system to provide good reproducibility of pulse parameters at the output of high-energy amplification cascades. It is planned to achieve this, on the one hand, due to the wide application of commercially available fibre and solid-state amplifiers from the best manufacturers and, on the other hand, by enclosing newly developed optical units in individual housings, with application of thermal and active stabilisation. The expected values of the output parameters of the front-end system are listed in Table 1.

The front-end system will be also equipped with several auxiliary beam outputs, which can be used in related experimental setups entering the XCELS project. For example, a picosecond pulse at $\lambda = 1030$ nm can be used to design a laser irradiating the electron accelerator photocathode [18] when studying the interaction of high-power laser radiation with electron beams. A CEP stabilised pulse with a width of few field oscillations can be used in attosecond physics research [19]. A nanosecond pulse at $\lambda = 1054$ nm can be applied (after amplification) in experiments requiring simultaneous use of nano- and femtosecond pulses (see, e.g., [5]). All these studies call for optical synchronisation of signals with all devices of the XCELS complex.

3. Design of front-end laser system

One should apply the most up-to-date and promising methods to achieve the parameters listed in Table 1. For example, stringent requirements to the time jitter lead to necessity of optical synchronisation of the output channels of the front-end system. The requirements to the temporal stability of output channels can be fulfilled by applying diode pumping of solid-state amplifiers. Diode pumping will also ensure a high repetition rate of solid-state amplifier output pulses, which is

Table 1. Main parameters of the XCELS front-end part.

Outputs	Wavelength/nm	Bandwidth (FWHM)/nm	Energy/mJ	Duration	Pulse repetition rate	Error in synchronisation with external clock/ps	Output energy stability (standard deviation) (%)
Femtosecond channel	910	~100	>100	~3 ns*	>10 Hz	<1	0.5
Pump channel for intermediate OPCPA (DKDP-1)	1054	0.05–3	>100	~4 ns	>2 Hz	<10	0.5
Two pump channels for power OPCPA (DKDP-0-12)	1054	0.05–3	>100	~4 ns	>2 Hz	<10	0.5
Auxiliary channel 1 (nanosecond)	1054	~1	~0.001	~1 ns	100 kHz	<1	0.3
Auxiliary channel 2 (picosecond)	1030	~1	~0.001	1 ps	50 MHz	<1	0.3
Auxiliary channel 2 (femtosecond)	910	>200	1	15 fs	1 kHz	<1	1

*Duration after the compressor is less than 15 fs; the contrast is better than 10^{14}.

important for carrying out preliminary diagnostics and aligning the main part of XCELS. To obtain a broadband femtosecond signal, one must apply different methods of nonlinear spectral broadening and field phase stabilisation relative to the envelope. Time shaping of laser pulse with a subnanosecond resolution is necessary to compensate for the pulse shape distortion in Nd:glass power amplifiers in the main part of XCELS. In this section we describe the fundamental approaches and specific solutions taken as a basis in developing the front-end system.

The front-end system (Fig. 2) can be arbitrarily divided into fibre, solid-state, and parametric parts. The fibre part provides synchronisation of optical pulses relative to an external frequency standard signal and forms master pulses at the fundamental wavelengths used in the XCELS laser. Optimal temporal and spatial profiles of pump pulses are formed, and these pulses are amplified to corresponding energies in the solid-state part. Parametric generation of femtosecond pulses and their amplification (with a high contrast provided) are performed in the parametric part.

3.1. Fibre part

The fibre-part functional design is presented in Fig. 2a. Here, the master oscillator (MO) is a femtosecond ytterbium fibre laser with a pulse repetition rate of several tens of MHz, synchronised with an external frequency standard. This configuration makes it possible to synchronise all devices necessary for experiments with the pulses at the XCELS output. The MO beam is split into two replicas. One of them is stretched in a fibre stretcher (FS), based on a fibre Bragg grating, to ~1 ns and amplified in a fibre amplifier FA1 at $\lambda \sim 1030$ nm to an energy of several tens of nJ. Then the pulse is divided into three replicas. An electro-optic filter (EOF) (aimed at reducing the pulse repetition rate) and a delay line (DL) based on a piezoelectric wafer [20] (aimed at performing precise time delay alignment) are installed in the path of each replica. Two of these replicas will be used in the ytterbium-doped fibre amplifiers of the solid-state part (Fig. 2b), and the third will play the role of auxiliary output 2.

The second replica of MO radiation will be compressed to a transform limited duration and introduced into a nonlinear fibre (NLF), which should broaden the spectrum so as to make it overlap the Nd:glass gain bandwidth. The pulse duration for femtosecond fibre oscillators is generally ~100 fs or less, due to which the high coherence of radiation is retained after nonlinear interaction with a fibre. Then the pulse is divided into four replicas; each will be amplified to several tens of nJ in fibre regenerative amplifiers FRA1–FRA4. DLs and acousto-optic filters (AOFs) [21] will be installed before each FRA; the former will be used to align pulse delays in the picosecond range, and the latter will change the spectral width of the transmitted beam from several nanometres to several tenths of nanometre, with an envelope shape close to Gaussian.

A chirping fibre Bragg grating (CFBG) is used as one of FRA cavity mirrors. The injection and extraction of radiation are performed with the aid of EOF and a Faraday isolator (FI). Multiple reflection from a CFBG with a dispersion of ~100 ps nm^{-1} and a width of reflection spectrum of more than 5 nm should provide necessary stretching, even for narrowband signals with a spectral width less than 0.1 nm, and make it possible to control relatively gradually the duration of pulses with a spectral width of ~1 nm by varying the number of FRA bypasses. A simultaneous adjustment of pump power will ensure conservation of pulse energy at the level of 100 nJ for any number of bypasses. The characteristic expected spectrum and pulse shape for parametric pumping of channels, implemented in commercially available laser system Avesta, are presented in Fig. 3. The reproducibility of measurement results is very high (better than 0.3% of standard deviation), and the small modulation of distributions depends in many respects on the way of radiation injection into measuring fibre devices. The proposed concept of the fibre part of front-end system will make it possible to control instrumentally the duration and spectral width in wide ranges, without any interference into design. The FRA1 output pulse will be used as an auxiliary channel, and three other FRAs will serve for injection into Nd:glass amplifiers of the solid-state part.

Note that the proposed design of the fibre part is based on standard solutions and components and can was implemented using commercial products from leading laser technique manufacturers.

One of important tasks of the front-end part is to implement a sufficiently high degree of synchronisation between the femtosecond and pump signals during further parametric amplification of pulses. One of the well-known approaches

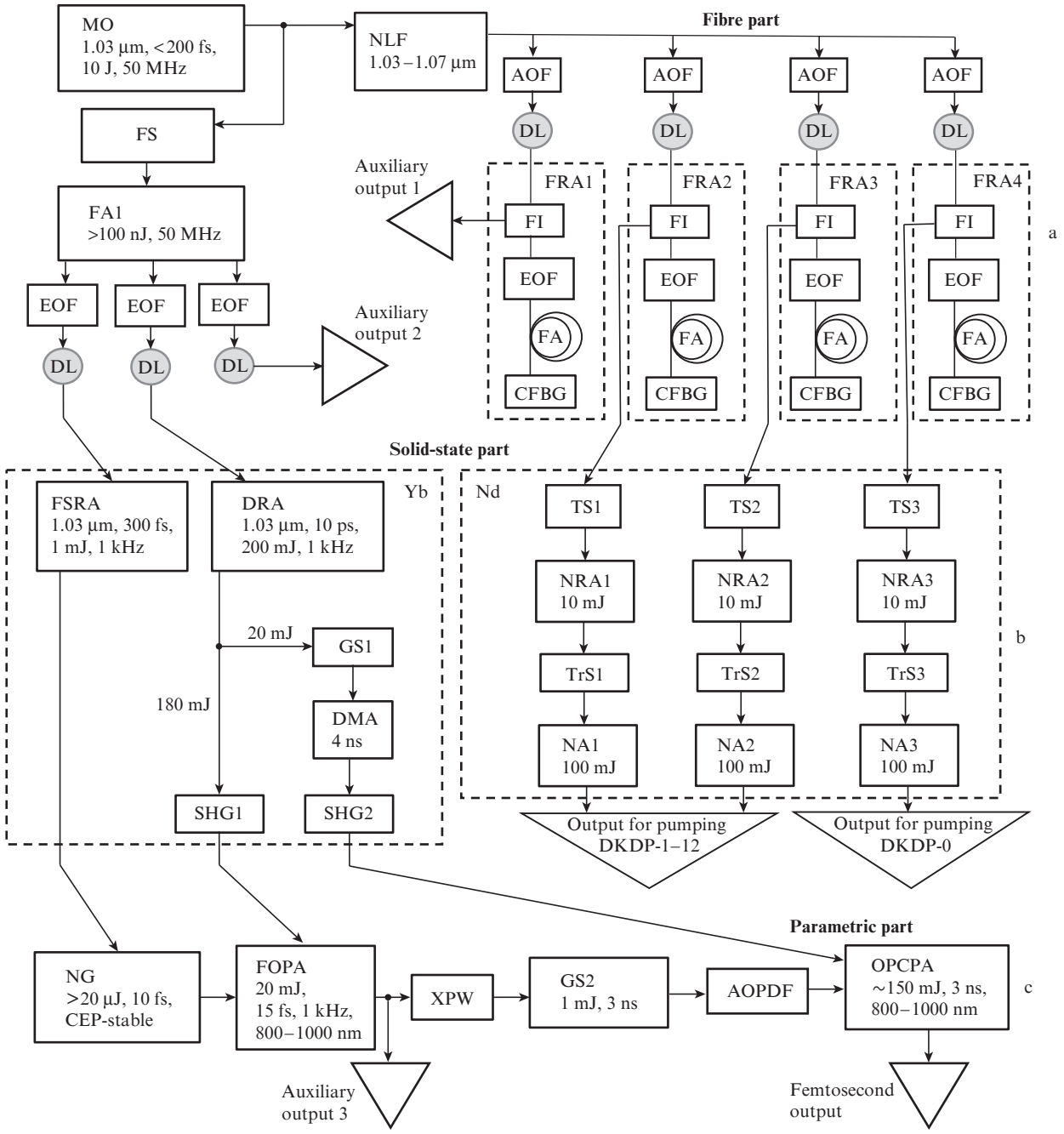

Figure 2. Functional scheme of the (a) fibre, (b) solid-state, and (c) parametric parts of the front-end system: (MO) master oscillator; (NLF) nonlinear fibre for spectral broadening; (FA) fibre amplifier; (AOF) acousto-optic filter; (EOF) electro-optic filter; (DL) delay line based on a piezoelectric wafer; (FI) Faraday isolator; (CFBG) chirping fibre Bragg grating; (FRA1–FRA4) fibre regenerative amplifiers; (FSRA) femtosecond regenerative amplifier; (DRA) disk regenerative amplifier; (DMA) disk multipass amplifier; (TS1–TS3) pulse time shaping units; (TrS1–TrS3) laser beam transverse shaping units; (NRA1–NRA3) neodymium regenerative amplifier; (NA1–NA3) neodymium rod amplifiers; (NG) unit for nonlinear parametric generation of broadband femtosecond radiation; (SHG1; SHG2) second-harmonic generation units; (FOPA) frequency domain optical parametric amplification unit; (XPW) cross-polarised wave generation unit; (OPCPA) optical parametric chirped-pulse amplification unit; (FS) fibre stretcher; (GS1–GS2) diffraction grating stretchers; (AOPDF) acousto-optic programmable dispersion filter.

used to this end is optical synchronisation, at which the initial radiation of synchronised signals is generated in a unified femtosecond optical oscillator. As will be shown below, the generation of femtosecond signal will be performed via nonlinear signal conversion after one of ytterbium solid-state amplifiers (Yb amplifiers based on a Yb:YAG crystal), and the pump signal will be prepared in Nd amplifiers. The optical signal for amplifiers of both types is generated in a unified femtosecond fibre oscillator. Due to the high pulse repetition rate for all output signals of the fibre part, one can choose pulses differing in time for amplification in order to minimise the time delay between emission pulses in different channels. All these pulses are mutually optically synchronised, because they are replicas of the same pulse generated in the femtosecond oscillator, with a time delay relative to each other corresponding to the femtosecond source cavity length.

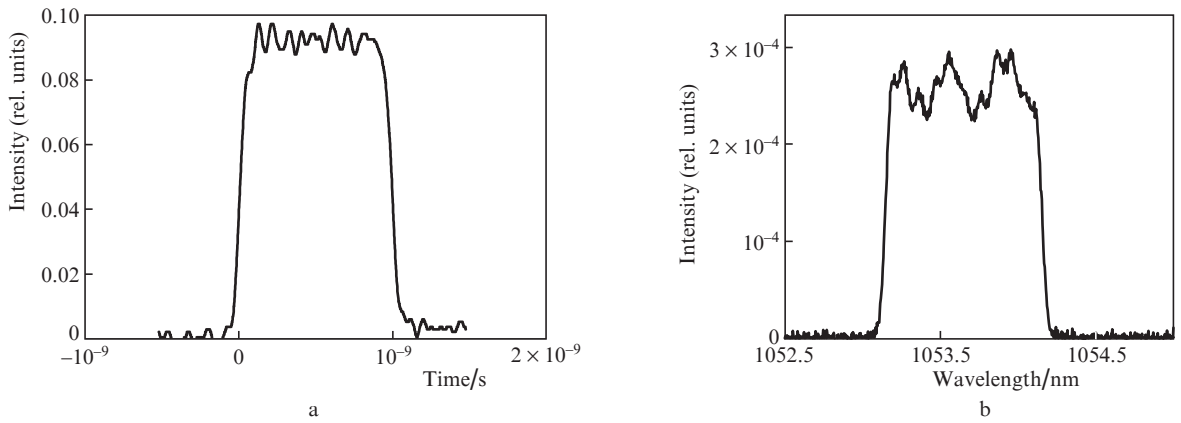

Figure 3. (a) Shape and (b) spectrum of a pulse from a prototype of fibre laser system (measurement by the scanning method). The pulse duration in the XCELS will be 5 ns.

Synchronisation with other devices can be implemented using the optical signal of auxiliary radiation outputs or synchronisation of the femtosecond fibre oscillator with an external frequency standard.

3.2. Solid-state part

The pulses from the fibre part output are amplified in the solid-state part (Fig. 2b). Two of them are amplified in Yb amplifiers, and three are amplified in Nd amplifiers. The femtosecond regenerative Yb amplifier FRA [22, 23] amplifies a pulse to a millijoule energy level with conservation of minimum (subpicosecond) duration. This pulse is used in the parametric part to generate a signal in the vicinity of 910 nm. The pulse from the second output of the fibre part will be amplified in an Yb disk regenerative amplifier (DRA), similar to that described in [24], to an energy of 200 mJ with a repetition rate of ~1 kHz and compressed to ~10 ps. Most of the pulse energy (180 mJ) will be used (after frequency doubling in SHG1) for picosecond pumping with frequency domain optical parametric amplification (FOPA) in the parametric part (see Fig. 2b). The rest of the pulse (20 mJ) will be stretched to 5 ns in the grating stretcher GS1 and amplified in a disk multipass amplifier DMA to subjoule energy (repetition rate ~100 Hz). This pulse, after doubling in SHG2, will be applied for nanosecond pumping of OPCPA in the parametric part. The temporal shape of amplified laser pulse in Yb amplifiers will be close to Gaussian. The spatial shape of the laser beam after DMA will be transformed into super-Gaussian [25].

One of difficult-to-implement requirements to the front-end system is to provide a high signal repetition rate with relatively high pulse energy. Nd:YAG crystals are used to increase the pulse repetition rate in commercially available femtosecond systems with multiterawatt peak power [26]. However, the emission spectrum of this material is too narrow for chirped pulse amplification, and, using electrical synchronisation of pump and femtosecond pulses, one cannot satisfy the requirements to synchronisation. Therefore, an Yb:YAG crystal was chosen, for which the gain spectrum width exceeds 1 nm. To provide a high pulse repetition rate, it is planned to use an active element with disk geometry. As calculations showed, the use of a disk active element at pump energy of 4 J should provide up to 1 J accumulated energy and a gain of 1.5, while an application of an active element of composite structure [27] should yield energy up to 1.5 J and a gain of 2. In the multipass amplification scheme (which was investigated, e.g., in [28]), pulse energies at the subjoule level can be achieved at pulse energies of several tens of millijoules at the amplifier input.

The pulses from three 'neodymium' outputs of the front-end system, with a wavelength lying in the gain band of neodymium phosphate glass (1054 nm) and an adjustable spectral width, will be supplied to the systems of pulse temporal shaping TS1–TS3, whose action is based on spectral approaches. An important advantage of the use of chirped pump pulses (spectrons) is the possibility of controlling their temporal shape by modifying their spectra, as in [29, 30]. It is proposed to implement shaping in a scheme based on a stretcher–compressor system with zero frequency dispersion and a spatial light modulator (SLM) located in the compressor Fourier plane. This scheme was tested experimentally. The radiation source was a low-power cw diode laser with a centre wavelength of 1054 nm and a spectral width of several nanometres. An image in the form of 256 shades of gray, which are linearly related to the SLM-generated phase shift, is supplied to the SLM. A uniform change in the shades of gray leads to a change in the total transmission of the system, and spectral and temporal pulse modulation is implemented when a certain pattern is formed (for example, a 'window' with differing grades). The minimum transmittance of the system (1.2%) determines the maximum possible pulse modulation depth when passing through the shaping system (Fig. 4a). The range of values near the minimum width of transmission window (provided that the transmittance is no less than 50%) demonstrates a spectral resolution of the shaping system of about 0.12 nm (Fig. 4b). An increase in the diffraction grating groove density and/or beam diameter in the shaping system should improve additionally the spectral resolution.

Figure 5 shows the results of numerical simulation of the operation of the shaping system and amplifier. A 3-ns chirped Gaussian pulse (centre wavelength 1054 nm and spectral FWHM 1 nm) was used as the initial one. Then the shaper operation was simulated with allowance for the aforementioned resolution (120 pm pixel^{-1}). The spectral mask was chosen so as to make the laser pulse at the shaper output provide a quasi-rectangular temporal intensity distri-

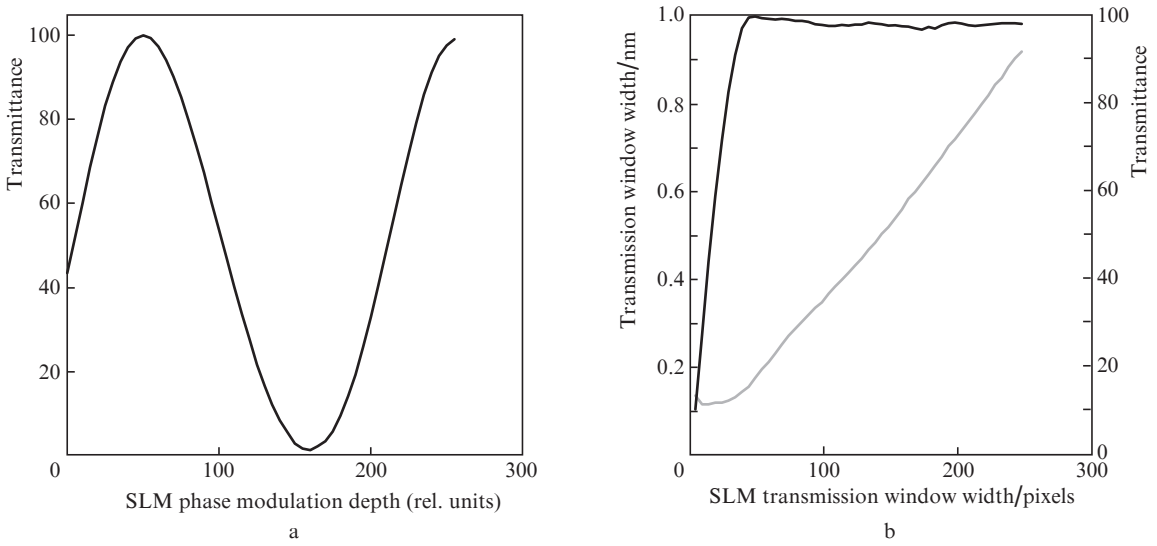

Figure 4. (a) Dependence of the shaping system transmittance in the 1-nm-wide working wavelength range on the SLM phase modulation depth and (b) dependences of the spectral width of transmission window (grey curve) and signal transmittance (black curve) on the width of the shaping system transmission window modulated on SLM.

bution with a duration of 4 ns at the amplifier output. The amplifier operation was simulated using the optical pumping scheme of the PEARL laser complex [15]. Curve *3* in Fig. 5 is the profile of a laser pulse with an energy of 300 J at the amplifier output.

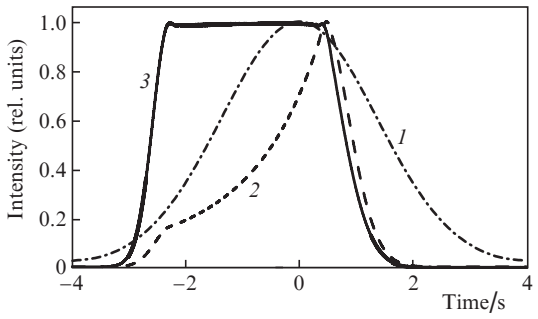

Figure 5. Shapes of pulses obtained by numerical simulation of the operation of shaping system and amplifier: (*1*) initial pulse, (*2*) shaped pulse, and (*3*) pulse at the amplifier output.

After temporal shaping, all three pulses are amplified to energy of ~10 mJ in Nd regenerative amplifiers NRA, which operate under weak-saturation conditions to minimise variations in the pulse shape. Regenerative amplifiers reduce also the pulse repetition rate to 10 Hz, with optimal time delay with respect to the femtosecond signal. Then the beam is transformed into the optimal transverse shape in the transverse shaping unit and amplified to an energy of more than 100 mJ in two-cascade rod Nd amplifiers NA1–NA3. Diode pumping in these amplifiers should make it possible to operate at a pulse repetition rate of 10 Hz. Then the pulses are injected into Nd:glass power amplifiers.

3.3. Parametric part

Chirped pulses with duration of ~4 ns are proposed to pump parametric amplification cascades both in the front-end system and in the entire XCELS facility. However, the presence of chirp may affect the parametric gain bandwidth in a nonlinear crystal. The influence of the pump pulse spectral width on the spectral dependence of parametric gain was numerically simulated. Calculations were performed for plane waves, with diffraction disregarded. The diffraction angle for beams of large diameter is much smaller than the experimental error in determining the phase-matching angle, which amounts to 0.02° [7]. The divergence of both the signal and pump beams is close to the diffraction divergence. Therefore, diffraction effects cannot affect essentially the gain bandwidth. Figure 6 shows the spectral dependences of gain in a 68-mm-long DKDP crystal with a degree of deuteration of 96% under monochromatic pumping with a wavelength of 527 nm [7] and under frequency-chirped pumping with a chirp sign coinciding the signal chirp sign or having an opposite value. In all cases the pump intensity was 1 GW cm^{-2}, and the interaction angles were slightly varied near the phase-matching angle at the centre pump and signal wavelengths in order to optimise the gain band. It can be seen in Fig. 6 that, fitting the interaction angles, one can provide signal amplification in the desired band to 200 nm, independent of the pump chirp sign. Thus, the use of chirped pump pulses may slightly shift the gain band or increase its width, which does not affect much the parametric amplification efficiency.

The radiation source for the signal wave of the parametric part of the front-end system will be a millijoule-level signal from the ytterbium FRA output. As in [31, 32], this radiation will be converted (using supercontinuum generation and parametric amplifiers) into the wavelength range of 700–1000 nm, with a transform limited duration of several field oscillations and passive stabilisation of field oscillation phase relative to the envelope, which may be important for implementing coherent combining of 12 XCELS laser pulses at the interaction point. The possibility of broadband generation of femtosecond radiation in this system was investigated experimentally in [32]. The spectrum of the radiation emitted by the laser system described in [32] is in the vicinity of 2 μm. This system was somewhat upgraded: the centre radiation

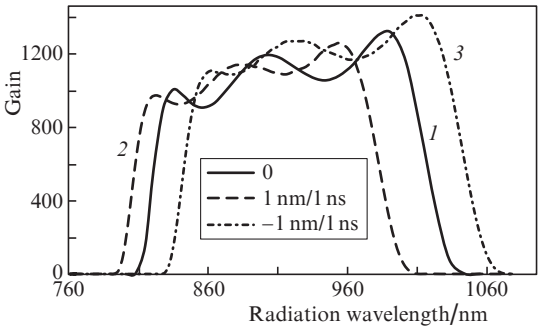

Figure 6. Spectral dependences of gain in a DKDP crystal: (*1*) under monochromatic pumping at $\lambda = 527$ nm (the deviation of the angle in the critical plane between the pump wave vector and the crystal optical axis from the exact phase-matching angle is $\Delta\theta_3 = -0.045°$, the deviation angle in the noncritical plane between the pump wave vector and signal wave vector from the exact phase-matching angle is $\Delta\varphi_{13} = -0.052°$), (*2*) under frequency-chirped pumping (1 nm/1 ns) with a chirp sign coinciding with the signal chirp sign ($\Delta\theta_3 = -0.133°$, $\Delta\varphi_{13} = -0.167°$), and (*3*) under frequency-chirped pumping (1 nm/1 ns) with a chirp sign opposite to that of signal ($\Delta\theta_3 = 0.076°$, $\Delta\varphi_{13} = 0.083°$). The exact phase-matching angles are $\theta_3 = 37.03°$ and $\varphi_{13} = 0.91°$ [7].

wavelength was converted to the range of 1.8 μm by aligning the orientations of nonlinear crystals; a fairly thin BBO crystal was placed at the output for second-harmonic generation, then this signal was additionally parametrically amplified to 10 μJ and compressed to a transform limited duration by chirping mirrors. The first experiments showed that laser pulses with duration of ~20 fs (Fig. 7) can be generated in the parametric-gain band of the DKDP crystal. The experimentally obtained compression of signal to a duration close to transform limited one (~20 fs) indicates that this signal can be used for OPCPA amplification. The presence of two humps in the spectrum is due to the fairly complex scheme of generation of a femtosecond signal, which includes several nonlinear conversions. Aligning the crystals and varying the delay line length, one can control the width of the generated spectrum and the depth of the central dip. During further amplification of chirped femtosecond signal, the presence of a dip may partially compensate for the spectrally nonuniform parametric amplification if a pump pulse with a Gaussian (or bell-shaped) temporal shape is used. This approach will make it possible to reduce signal narrowing during further parametric amplification.

Then the pulse will be parametrically amplified in a BBO crystal (cut so as to implement type-I phase matching), with application of FOPA [33]. Pumping will be performed by the second harmonic from the output of disk regenerative amplifier DRA1 (see Fig. 2). This approach will make it possible to avoid additional stretching and compression units in this stage of signal amplification. At an FOPA optical efficiency of 10%, the amplified pulse energy will be ~18 mJ. Note that optical synchronisation will provide subpicosecond time jitter between the signal and pump beams, even without additional pulse stabilisation [34]; the measures taken for time stabilisation should reduce jitter to several tens of femtoseconds [35]. To provide stable amplification in the FOPA, the pump pulse duration should be an order of magnitude larger (~10 ps). According to preliminary calculations, the FOPA approach can be scaled and optimised so as to make it possible to use an ytterbium laser as a pump source and a signal pulse with a duration of ~10 ps. Using pump energy of ~200 mJ, available-to-date BBO crystals with an aperture of ~30 mm, and a diffraction grating with a density of 300 grooves mm^{-1}, one can efficiently amplify radiation with a spectral width of ~300 nm.

To increase the contrast of the femtosecond pulses produced by the front-end system, it is planned to implement the method of cross-polarised wave (XPW) generation [36] at the millijoule level of signal energy. Note also that the use of picosecond pumping in previous amplification cascades will make it possible to exclude deterioration of femtosecond pulse contrast in the nanosecond time interval.

Then the signal pulse with a spectrum optimal for further amplification will be stretched by a stretcher based on a diffraction grating (PC2 in Fig. 2). Obviously, to implement

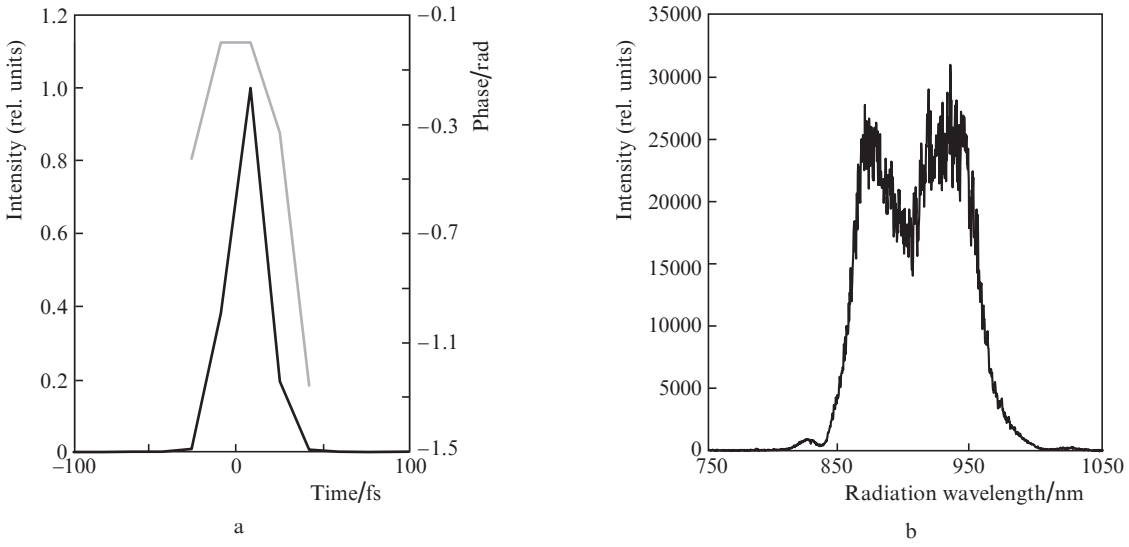

Figure 7. (a) Shape and phase (gray curve) of a pulse, measured by the FROG method and (b) spectrum of femtosecond radiation from a nonlinear parametric system [32] tuned to the central radiation wavelength: 910 nm.

matching in dispersion characteristics, the stretcher and compressor should be based on diffraction gratings of identical groove density and have close angles of beam incidence on gratings. The large diameter of beams in the compressor (from 40 to 55 cm) and a fairly wide spectrum of signal beam impose limitations on the minimum distance between the compressor gratings, thus determining the minimum duration of stretched pulse. For beams with diameters of 1–2 cm, the pulse can easily be stretched to 3 ns. Note that, to minimise the aberrations of the stretcher, it is proposed to implement it in the Offner scheme with two diffraction gratings. Then this radiation will be directed to the acousto-optic programmable dispersive filter AOPDF [37] to optimise the spectral phase and achieve transform limited pulse duration after the final XCELS compressor.

A pulse transmitted through AOPDF is parametrically amplified in a DKDP crystal (OPCPA in Fig. 2), using the second harmonic from disk amplifier DMA for pumping. At second-harmonic pulse energy of 500 mJ and parametric amplification efficiency of ~30%, one would expect chirped femtosecond pulses to have energy of ~150 mJ and a high (up to 100 Hz) repetition rate. Then a pulse is directed to the power parametric amplifiers of the XCELS main part.

4. Conclusions

The results of preliminary studies and development of the conceptual design of laser system for the front-end system of XCELS subexawatt laser have been reported. The combination of fibre and solid-state parts of the laser system makes it possible to control flexibly the main parameters of output channels and use additional channels when necessary. Due to the approaches based on supercontinuum generation and passive CEP stabilisation, the femtosecond signal parameters can be tuned in a wide range. The application of picosecond cascades of parametric amplification and cross-polarised wave generation provides a high contrast of femtosecond pulses at the millijoule energy level. The generation of radiation with a relatively high average power in the channels of the front-end system should provide stabilisation of the main parameters of the final cascades of XCELS facility. Some of the main components of the front-end system are commercially available, the others are products of scientific research. Several proposed units and approaches have been either developed or experimentally verified by the authors of this study.

Acknowledgements. The work was supported by the World-Class Research Centre "Photonics Centre" under the financial support of the Ministry of Science and High Education of the Russian Federation (Aagreement No. 075-15-2020-906) and the European Commission (Grant No. 71072-CREMLINplus).

References

1. Zeng X., Zhou K., Zuo Y., Zhu Q., Su J., Wang X., Wang X., Huang X., Jiang X., Jiang D., Guo Y., Xie N., Zhou S., Wu Z., Mu J., Peng H., Jing F. *Opt. Lett*., **42** (10), 2014 (2017).
2. Thales website: https://www.thalesgroup.com/en/group/journalist/press release/worlds-most-powerful-laser-developed-thales-and-eli-np-achieves.
3. Perry M.D., Pennington D., Stuart B.C., Tietbohl G., Britten J.A., Brown C., Herman S., Golick B., Kartz M., Miller J., Powell H.T., Vergino M., Yvanovsky V. *Opt. Lett*., **24** (3), 160 (1999).
4. Albach D., Loeser M., Siebold M., Schramm U. *High Power Laser Sci. Eng.*, **7**, e1 (2019).
5. Ren J., Cheng W., Li S., Suckewer S. *Nature Phys*., **3** (10), 732 (2007).
6. Khazanov E.A., Mironov S.Yu., Mourou G. *Phys. Usp.*, **62**, 1096 (2019) [*Usp. Fiz. Nauk*., **189** (11) 1173 (2019)].
7. Lozhkarev V.V., Freidman G.I., Ginzburg V.N., Khazanov E.A., Palashov O.V., Sergeev A.M., Yakovlev I.V. *Laser Phys*., **15** (9), 1319 (2005).
8. Bromage J., Bahk S.-W., Begishev I.A., Dorrer C., Guardalben M.J., Hoffman B.N., Oliver J.B., Roides R.G., Schiesser E.M., Shoup M.J. III, Spilatro M., Webb B., Weiner D., Zuegel J. *High Power Laser Sc. Eng.*, **7**, e4 (2019).
9. Kawanaka J., Tsubakimoto K., Yoshida H., Fujioka K., Fujimoto Y., Tokita S., Jitsuno T., Miyanaga N., Team G.-E.D. *J. Phys.: Conf. Ser*., **688**, 012044 (2016).
10. Beijie Shao, Yanyan Li, Wenkai Li, Yujie Peng, Pengfei Wang, Junyu Qian, Yuxin Leng, Li R., in *Techn. Dig. The 22nd International Conference on Ultrafast Phenomena* (OSA. 2020) paper W2A.7.
11. Zhu J., Xie X., Sun M., Kang J., Yang Q., Guo A., Zhu H., Zhu P., Gao Q., Liang X., Cui Z., Yang S., Zhang C., Lin Z. *High Power Laser Sci. Eng*., **6** (29), 1 (2018).
12. https://xcels.iapras.ru.
13. Gonoskov I., Aiello A., Heugel S., Leuchs G. *Phys. Rev. A*, **86**, 053836 (2012).
14. Tesar A., Campbell J., Weber M., Weinzapfel C., Lin Y., Meissner H., Toratani H. *Opt. Mater.*, **1** (3), 217 (1992).
15. Shaykin A.A., Kuzmin A.A., Shaikin I.A., Burdonov K.F., Khazanov E.A. *Quantum Electron*, **46** (4), 371 (2016) [*Kvantovaya Elektron*., **46** (4), 371 (2016)].
16. https://amplitude-laser.com/products/nanosecond-lasers/nanosecond-advanced-lasers/premiumlite-glass/.
17. https://scientificrussia.ru/articles/samaya-moshchnaya-lazernaya-ustanovka-v-mire-stroitelstvo-ufl-2m-v-sarove.
18. Mironov S.Yu., Andrianov A.V., Gacheva E.I., Zelenogorskii V.V., Potemkin A.K., Khazanov E.A., Boonpornprasert P., Gross M., Good D., Isaev I., Kalantaryan D., Kozak T., Krasilnikov M., Qian H., Li X., Lishilin O., Melkumyan D., Oppelt A., Renier Y., Rublack T., Felber M., Huck H., Chen Y., Stephan F. *Phys. Usp.*, **60**, 1039 (2017) [*Usp. Fiz. Nauk*., **187** (10), 1121 (2017)].
19. Corkum P.B., Krausz F. *Nature Phys*., **3**, 381 (2007).
20. Zelenogorskii V.V., Andrianov A.V., Gacheva E.I., Gelikonov G.V., Krasilnikov M., Mart'yanov M.A., Mironov S.Yu., Potemkin A.K., Syresin E.M., Stephan F., Khazanov E.A. *Quantum Electron*., **44** (1), 76 (2014) [*Kvantovaya Elektron*., **44** (1), 76 (2014)].
21. https://www.santec.com/en/products/instruments/tunablefilter/?gclid=Cj0KCQjwnueFBh ChARI%20sAPu3YkRN6Y5y_.
22. http://avesta.ru/en/product/teta-industrial-femtosecond-laser-system/.
23. https://lightcon.com/product/pharos-femtosecond-lasers/.
24. https://www.trumpf-scientific-lasers.com/products/dira-series/.
25. http://www.pishaper.com/.
26. Budriūnas R., Stanislauskas T., Adamonis J., Aleknavičius A., Veitas G., Gadonas D., Balickas S., Michailovas A., Varanavičius A. *Opt. Express*, **25** (5), 5797 (2017).
27. Vadimova O., Kuznetsov I., Mukhin I., Perevezentsev E., Palashov O. *Laser Phys*., **25**, 095001 (2015).
28. Chen H., Song E., Dong J., Zhu X., Wang H., Zhu G., in *Techn. Dig. Conference on Lasers and Electro-Optics (*OSA 2020) paper JW2B.13.
29. Mironov S.Y., Poteomkin A.K., Gacheva E.I., Andrianov A.V., Zelenogorskii V.V., Krasilnikov M., Stephan F., Khazanov E.A. *Appl. Opt*., **55** (7), 1630 (2016).
30. Kuzmin I., Mironov S., Gacheva E., Zelenogorsky V., Potemkin A., Khazanov E., Kanareykin A., Antipov S., Krasilnikov M., Loisch G. *Laser Phys. Lett*., **16** (1), 015001 (2019).
31. Chen P.-Y., Farhat M., Askarpour A.N., Tymchenko M., Alù A. *Optics*, **16**, 094008 (2014).

32. Mukhin I.B., Volkov M.R., Vikulov I.A., Perevezentsev E.A., Palashov O.V. *Quantum Electron*., **50** (4), 321 (2020) [*Kvantovaya Elektron*., **50** (4), 321 (2020)].
33. Schmidt B.E., Thire N., Boivin M., Laramee A., Poitras F., Lebrun G., Ozaki T., Ibrahim H., Legare F.O. *Nature Commun*., **5**, 3643 (2014).
34. Casanova A. et al. *Opt.Lett*., **41** (5), 898 (2016).
35. Miura T., Takasago K., Kobayashi K., Zhang Z., Torizuka K., Kannari F. *Jpn J. Appl. Phys. Pt 1*, **40**, 1260 (2001).
36. Ramirez L.P., Papadopoulos D.N., Pellegrina A., Georges P., Druon F., Monot P., Ricci A., Jullien A., Chen X., Rousseau J.P., Lopez-Martens R. *Opt. Express*, **19** (1), 93 (2011).
37. Tournois P. *Opt. Commun*., **140** (4–6), 245 (1997).